Hemodynamic fluctuations and baroreflex sensitivity in humans: a beat-to-beat model

R. W. DEBOER, J. M. KAREMAKER, AND J. STRACKEE
Department of Physiology and Laboratory of Medical Physics, University of Amsterdam, 1105 AZ Amsterdam, The Netherlands

DEBOER, R. W., J. M. KAREMAKER, AND J. STRACKEE. *Hemodynamic fluctuations and baroreflex sensitivity in humans: a beat-to-beat model.* Am. J. Physiol. 253 (Heart Circ. Physiol. 22): 680–689, 1987.—A beat-to-beat model of the cardiovascular system is developed to study the spontaneous short-term variability in arterial blood pressure (BP) and heart rate (HR) data from humans at rest. The model consists of a set of difference equations representing the following mechanisms: *1*) control of HR and peripheral resistance by the baroreflex, *2*) Windkessel properties of the systemic arterial tree, *3*) contractile properties of the myocardium (Starling's law and restitution), and *4*) mechanical effects of respiration on BP. The model is tested by comparing power spectra and cross spectra of simulated data from the model with spectra of actual data from resting subjects. To make spectra from simulated data and from actual data tally, it must be assumed that respiratory sinus arrhythmia at rest is caused by the conversion of respiratory BP variability into HR variability by the fast, vagally mediated baroreflex. The so-called 10-s rhythm in HR and BP appears as a resonance phenomenon due to the delay in the sympathetic control loop of the baroreflex. The simulated response of the model to an imposed increase of BP is shown to correspond with the BP and HR response in patients after administration of a BP-increasing drug, such as phenylephrine. It is concluded that the model correctly describes a number of important features of the cardiovascular system. Mathematical properties of the difference-equation model are discussed.

blood pressure fluctuations; heart rate variability; cardiovascular system; mathematical modeling; spectral analysis; power spectra; cross spectra; respiratory sinus arrhythmia; 10-s variability; Mayer waves

THE HEART IS NOT a continuous pump but acts in a discrete fashion with the successive heartbeats leading to a series of fluctuating values of R-R intervals and systolic and diastolic pressures. Still, almost all models of the cardiovascular system (CVS) consist of sets of differential equations, representing relationships between continuous signals such as mean arterial blood pressure (BP) and heart rate (HR) (for a recent review see Ref. 5). If one is only interested in the long-term regulation of the CVS, this neglect of the pulsatile character of the heartbeat seems justified. However, as we wish to study the relationship between short-term fluctuations in BP and HR, we have developed a beat-to-beat model of the human CVS based on physiological considerations. The model can be used to obtain simulated BP data and R-R interval data, both for subjects at rest and after the administration of a vasoconstricting, hence BP-increasing, drug (e.g., phenylephrine). The performance of the model is assessed by comparison of simulated data and actual human data.

In resting humans, beat-to-beat fluctuations in BP and HR are mainly due to respiratory influences and to the slower Mayer waves (for a review see Ref. 23). The fastest and often the most conspicuous Mayer waves constitute the so-called 10-s rhythm, having a period of ~10 s (13). One of the purposes of our study is to obtain information about the functioning of the CVS under normal physiological conditions from the relationship between these spontaneous BP and HR fluctuations, thus dispensing with the need for pharmacological or other interventions.

We use spectral-analysis techniques to differentiate between fluctuations due to the 10-s rhythm (at ~0.1 Hz) and due to respiratory influences (usually 10–20 breaths/min or 0.15–0.35 Hz). Examples of power spectra and cross spectra of HR variability and BP variability from healthy human subjects at rest were presented in a previous paper (9). At that time we gave only a partial interpretation of these spectra, using a very simple beat-to-beat model of the CVS (10). This old model was not able to explain the shape of the phase spectrum of systolic pressure variability against interval variability that was obtained from actual data. It was then found that the phase spectrum derived from the model and the phase spectrum computed from actual data agreed only for respiratory frequencies (0.2–0.35 Hz), but at the frequency of the 10-s rhythm the old model predicted a phase difference of 0° (pressure and interval in phase), whereas the experimental data show a phase difference of ~−70° (pressure leads interval). It will be shown that the present model greatly improves on these results (see *Simulation of Resting Data*).

The results of our simulations suggest that respiratory

sinus arrhythmia is caused by the respiratory BP waves and not vice versa (for a review see Ref. 25). It also appears possible to simulate realistic 10-s waves due to the delay in the sympathetic feedback loop of the baroreflex. The simulated waves resemble the actual ones both in visual appearance and in spectral properties (power spectra and cross spectra).

We also simulate the pressure and interval responses of the model to the administration of a BP-increasing drug, e.g., phenylephrine (see *Response to Simulated Phenylephrine Injection*). These responses are shown to correspond well with experimental data. Clinically a BP-increasing drug is administered to test the functioning of the baroreflex. The interval prolongation due to the BP increase has been used as a measure for the so-called baroreflex sensitivity (33).

The similarity of simulated data from the model and actual behavior of the CVS makes it tempting to believe that the mechanisms built into our model conform to the short-term control properties of the CVS.

The discrete beat-to-beat approach used for our model leads to a system of difference equations, whereas other published models of the CVS consider continuous variables and hence consist of systems of differential equations (2, 5, 14, 15, 36). Some mathematical properties of our difference-equation model are discussed in the APPENDIX. Preliminary results were presented before (6, 19).

DESCRIPTION OF THE MODEL

The model we present is a beat-to-beat model in which the features of each heartbeat (e.g., systolic pressure, length of the interbeat interval) depend on the features of previous beats. The following properties of the CVS are included in the model: *1*) control of interbeat interval and of peripheral resistance by the baroreflex, *2*) Windkessel properties of the systemic arterial tree, *3*) contractile properties of the myocardium (Starling's law and restitution properties), and *4*) mechanical effects of respiration on BP.

The model is an extension of the beat-to-beat model presented previously (7, 10). It may be visualized by the diagram of Fig. 1. The BP value is sensed by the baroreceptors, and accordingly, the central nervous system adjusts the heart rate by both fast vagal action and by slower sympathetic action (baroreflex control of HR). The baroreflex also affects the peripheral resistance but only via sympathetic efferent activity. The heart rate (or equivalently the length of the R-R interval) influences the cardiac output, which together with the peripheral resistance determines the value of BP and thus closes the loop. For reasons to be discussed later, respiration is assumed to affect first the cardiac output and hence BP and subsequently the R-R interval via the baroreflex. Note that the model equates the P-P intervals, which originate from the pacemaker, with the R-R intervals, which determine the cardiac output. The model is meant to cover only relatively fast fluctuations in BP and HR with periods of <20 s, i.e., frequencies >0.05 Hz. No slow regulatory mechanisms are included.

The present model differs from the one in Ref. 7 by

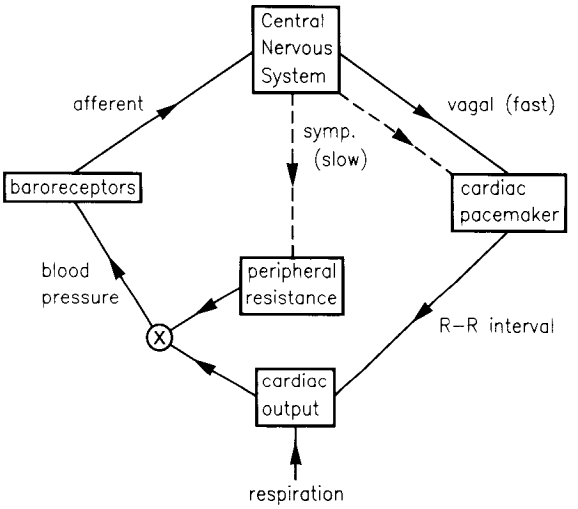

FIG. 1. Schematic diagram of cardiovascular system. Blood pressure (BP) affects, through baroreceptors and central nervous system, both interval length and peripheral resistance (baroreflex). *Dashed line* indicates slow sympathetic control. Cardiac output is determined by heart rate (or R-R interval). Peripheral resistance and cardiac output determine new BP value. Our simulations suggest that respiration first affects BP possibly through mechanical effects.

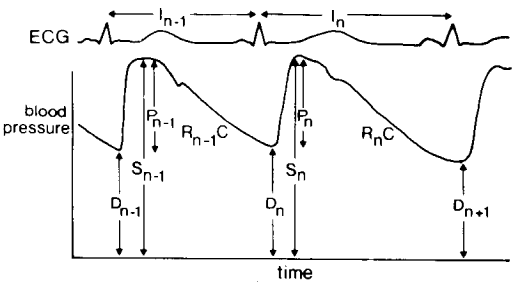

FIG. 2. Notations as used in this paper. Systolic pressure S_n, pulse pressure P_n, diastolic pressures D_n, and peripheral resistance R_n occur during R-R interval I_n. Product of peripheral resistance R_n and (supposedly constant) arterial compliance **C** gives time constant $T_n = R_nC$ of diastolic pressure decay. ECG, electrocardiogram.

the presence of sympathetic control of R-R interval and peripheral resistance. In the following we describe the new model in detail. It consists of a set of five difference equations. The notations used are shown in Fig. 2: systolic pressure (S_n), pulse pressure (P_n), diastolic pressure (D_n), and peripheral resistance (R_n) occur during R-R interval (I_n).

It is convenient to use operation points of pressure and interval variables because only small deviations from the operation points occur if the model is used to generate simulated data for a subject at rest. In that case the difference equations of the model may be linearized around these points, which considerably facilitates the analysis of the model. The operation points are indicated as systolic pressure (**S**), diastolic pressure (**D**), pulse pressure (**P**), peripheral resistance (**R**), R-R interval (**I**), and arterial time constant (**T** = **RC**) with **C** as the arterial compliance. The deviation s_n of the systolic pressure S_n from its operation point **S** is defined as $s_n = S_n - \mathbf{S}$. Similarly we define $d_n = D_n - \mathbf{D}$, $p_n = P_n - \mathbf{P}$, $r_n = R_n - \mathbf{R}$, $\tau_n = T_n - \mathbf{T}$, and $i_n = I_n - \mathbf{I}$. The operation points were chosen as **S** = 120 mmHg, **D** = 75 mmHg, **I** = 800 ms, and **T** = 1,425 ms. These are normal human values, the last one being taken from the model of Wes-

seling et al. (36) (cf. the values in Ref. 31). We give for each equation of the model both the full form and the linearized small-deviation form that may be used in the analysis of simulations for resting conditions (see APPENDIX).

Effective Pressure

Baroreceptors are known to respond proportionally in a limited range of systolic pressures only (24). Around the equilibrium pressure value the gain of the baroreflex is maximal, whereas for both low and high pressures the gain tends toward zero due to a threshold phenomenon and to saturation of the baroreceptors, respectively. This behavior is modeled by the concept of effective systolic pressure S'_n (and its deviation s'_n), which is a function of the actual pressure S_n

$$S'_n = F(S_n) \tag{1}$$

$$s'_n = f(s_n) \tag{1'}$$

The function F we used in the simulation is $F(S) = 120 + 18 \arctan [(S - 120)/18]$ or equivalently $f(s) = 18 \arctan(s/18)$. The sigmoidal shape of this function gives negligible differences between effective pressure S'_n and true pressure S_n for small (<10 mmHg) deviations from the operation point $\mathbf{S} = 120$ mmHg, whereas for high or low values of the systolic pressure the range of effective pressure remains limited to ~56 mmHg [cf. the "Blutdruck-Charakteristik" curves of Koch (22)].

Baroreflex on Heart Rate

The second equation represents the action of the baroreflex on the cardiac pacemaker

$$I_n = a_0 S'_n + \sum_{k>0} a_k S'_{n-k} + c_1 \tag{2}$$

$$i_n = a_0 s'_n + \sum_{k>0} a_k s'_{n-k} \tag{2'}$$

Equation 2 states that the length of the present interval I_n is determined both by the value of the (effective) systolic pressure S'_n during this interval (due to the fast vagal influence) and by a weighted sum of previous systolic values S'_{n-k}, representing the slower sympathetic influence (Fig. 3; cf. Ref. 3), plus some constant c_1.

The notations used in *Eq. 2* reflect the distinction between the vagal contribution a_0 and the sympathetic contributions a_k with $k > 0$. The value of the parameter a_0 is a measure of the vagal strength of the baroreflex arc, whereas the values of the parameters a_k with $k > 0$ determine the time response and strength of the sympathetically mediated control of interval length.

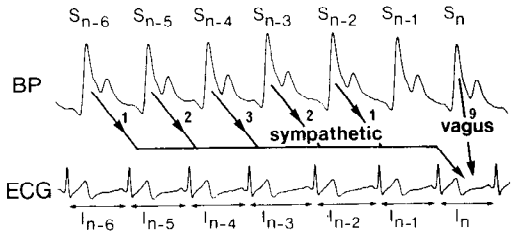

FIG. 3. Blood pressure (BP) registration and electrocardiogram (ECG), indicating control of cycle length by vagus nerves and sympathetic nerves. Interval length I_n is affected by systolic values S_n and S_{n-2} to S_{n-6}. I_n is not affected by S_{n-1} because vagal effect of S_{n-1} has already died out, and its sympathetic effect is not yet effective. *Numbers* indicate relative strength of influence of different systolic values on interval I_n as assumed in our model.

To obtain simulated data from our model, realistic values should be found for the parameters a_k. The overall strength of the baroreflex arc, the so-called baroreflex sensitivity (BRS), has been measured for clinical purposes by administering a pressure-increasing drug (e.g., phenylephrine) and by comparing the pressure-induced interval increase ΔI with the increase of pressure ΔBP (33). Values for the BRS, expressed as $\Delta I/\Delta BP$, are found as 10–20 ms/mmHg (29). The relative contributions of vagal and sympathetic activity to this overall value are not well known. Therefore we give in our model equal weight to the vagal and the sympathetic contribution, choosing a value of 9 ms/mmHg for the vagal parameter a_0. We take for the (sympathetic) a_ks a triangular weighting function, starting at a delay of two beats (around 2 s; cf. Ref. 3). The values of the a_ks were taken as $a_k = 1$, 2, 3, 2, and 1 ms/mmHg for $k = 2$, 3, 4, 5, and 6, respectively (see Fig. 3). In this way, the total sympathetic effect equals the vagal contribution. The results proved to be rather unsensitive to the exact shape of the weighting function.

Baroreflex on Peripheral Resistance

The next equation represents the sympathetic action of the baroreflex on the peripheral resistance R_n and hence on the time constant T_n of the arterial Windkessel (the arterial compliance $\mathbf{C}$ is assumed to be constant)

$$T_n(= R_n\mathbf{C}) = \mathbf{T}^* - \sum_{k>0} b_k S'_{n-k} \tag{3}$$

$$\tau_n(= r_n\mathbf{C}) = -\sum_{k>0} b_k s'_{n-k} \tag{3'}$$

According to *Eq. 3* the momentaneous value of R_n depends on a weighted sum of previous systolic values S'_{n-k} due to slow sympathetic influence (cf. *Eq. 2*). The minus sign is used because an increased pressure leads to a decrease of resistance. We take for the weighting coefficients b_k an identical triangular shape as for the sympathetic factors a_k in *Eq. 2*; good simulation results were obtained if the values were taken as $b_k = 2$, 4, 6, 4, and 2 ms/mmHg for $k = 2$, 3, 4, 5, and 6, respectively.

Properties of Myocardium

The influence of the length of the previous interval on the strength of the ventricular contraction is modeled by the following equation

$$P_n = \gamma I_{n-1} + c_2 \tag{4}$$

with $P_n = S_n - D_n$

$$p_n = \gamma i_{n-1} \tag{4'}$$

with $p_n = s_n - d_n$

Equation 4 states that a long interval I_{n-1} tends to increase the next pulse pressure P_n. This mechanism is assumed to be partly due to the increased filling of the

ventricles after a longer interval, which leads to a more forceful contraction (Starling's law), and partly to the restitution properties of the ventricular myocardium, which also leads to an increased strength of contraction after a longer interval. A numerical value for the parameter γ can be derived from experiments in which heart period is changed by atrial pacing, and the resulting change in ventricular contractile force is recorded. We used for our simulations a value of $\gamma = 0.016$ mmHg/ms, as did Wesseling et al. (36). This value is corroborated by experiments in both humans (30) and dogs (26).

Windkessel

The decrease of pressure during diastole is described by the Windkessel equation

$$D_n = c_3 \cdot S_{n-1} \exp(-I_{n-1}/T_{n-1}) \quad (5)$$

$$d_n = \mathbf{D}[s_{n-1}/\mathbf{S} - i_{n-1}/\mathbf{RC} + (\mathbf{I}/\mathbf{RC})\ \tau_{n-1}/\mathbf{RC}] \quad (5')$$

Due to the Windkessel properties of the arterial tree the value of the new diastolic pressure D_n depends on the value of the previous systolic pressure S_{n-1}, on the length of the preceding interval I_{n-1}, and on the value of the time constant $T_{n-1} = R_{n-1}\mathbf{C}$ of the Windkessel during the diastolic pressure decay. *Equation 5'* is derived from *Eq. 5* by assuming small deviations from the operation points **S**, **D**, **T**, and **I**.

The set of *Eqs. 1–5*, or equivalently *Eqs. 1'–5'*, constitutes a closed-loop model of the CVS: effective systolic values S'_{n-k} and S'_n (*Eq. 1*) determine a new value for R-R interval I_n and arterial time constant T_n (*Eqs. 2* and *3*). The combination of I_n, S_n, and T_n leads to a new value of the diastolic pressure D_{n+1} (*Eq. 5*); D_{n+1} and I_n combine to give the new systolic value S_{n+1} (*Eq. 4*); and so the loop is closed. The equations themselves do not imply any fluctuations in BP or HR but lead to stable values for the various variables.

RESULTS OF SIMULATIONS

Simulation of Resting Data

As a first test of the model simulated data are shown under steady-state conditions. To this end we must incorporate respiratory influence into the model either by assuming respiration to affect first BP and second the R-R interval by means of the baroreflex or else by assuming respiration to affect first the R-R interval and hence the blood pressure (cf. Fig. 1). In the former case respiration would enter the model through *Eq. 4* and in the latter case through *Eq. 2*. We found that an acceptable correspondence between power spectra and cross spectra from real data and from simulated data could only be found if the respiratory influence was included in *Eq. 4* (or *Eq. 4'*), which for this simulation was taken as

$$p_n = s_n - d_n = \gamma i_{n-1} + A \sin(2\pi\ f_{resp} \cdot \sum_k I_k) \quad (4'')$$

The last term represents the respiration with frequency f_{resp} and amplitude A. We chose A = 3 mmHg and $f_{resp} = 0.3$ Hz. The latter value corresponds with 18 breaths/min. $\sum_k I_k$ is the time of the kth beat. *Equation 4''* implies that the respiratory influence becomes first evident in the pulse pressures, possibly through the mechanical effects of breathing on stroke volume. The respiratory BP waves are subsequently converted into respiratory HR variability (the so-called respiratory sinus arrhythmia) by the baroreflex.

To make the model more realistic, noise was introduced into the system, i.e., random disturbances were added to *Eqs. 2'* and *4''* with independent Gaussian distributions, having means equal to zero and standard deviations 25 ms and 2 mmHg, respectively (36).

Actual BP and interval data from a 32-yr-old male subject at rest and simulated data are shown in Fig. 4, *A* and *B*, respectively. The data in Fig. 4*A* are from a subject whose blood pressure was measured by means of a noninvasive instrument developed by Wesseling and co-workers (see "Fin. A. Pres" in Ref. 35). Power spectra and cross spectra from these data are given in Fig. 2*A* in Ref. 9; there it is also shown that data from noninvasive Fin. A. Pres measurements and from intra-arterial measurements are comparable for all practical purposes. The data are representative for healthy subjects (9).

Both in the actual data (Fig. 4*A*) and in the simulated data (Fig. 4*B*) slow variability (10-s rhythm) and fast variability (respiration) can be observed in the systolic pressures and in the intervals; the diastolic pressures show only 10-s variability. The absence of respiratory variability in diastolic pressure values is explained in DISCUSSION. The simulated time constants T = RC (Fig. 4*B*) or, equivalently, the peripheral resistances also show only slow variability due to the low-pass filter characteristics of the sympathetic system (cf. *Eq. 3*). The actual data (Fig. 4*A*) and simulated data (Fig. 4*B*) look alike. A more critical comparison of the actual and simulated data can be made by consideration of power spectra and cross spectra of the data (Figs. 5 and 6).

Spectral Analysis of Pressure and Interval Data

Power spectra and cross spectra of pressure data and interval data were computed as described in detail in Ref. 9. In short, successive values of systolic, diastolic, and pulse pressures and of R-R intervals are taken to be equidistantly spaced, and spectra are then computed by a periodogram approach (discrete Fourier transform). The resulting frequency scale is in cycles per beat. It can be proven that if the deviations from the mean interval length are small this frequency scale may be converted into the usual cycles per second or Hz by assuming the spacing between successive beats to be equal to the mean interval length (8). The power spectra P(f) show the amount of variability as a function of frequency f and are therefore expressed either as s^2/Hz (interval spectrum, Figs. 5*A* and 6*A*) or as $mmHg^2$/Hz (pressure spectra, Figs. 5, *B* and *C* and 6, *B* and *C*). Note that the height of a spectral peak is not important, but only the total area under the peak.

The cross spectrum between, e.g., systolic pressure variability and interval variability consists of two parts (Figs. 5*D* and 6*D*). The (squared) coherence spectrum $k^2(f)$ (dashed line) shows the amount of linear relationship between the variability in the two signals at each

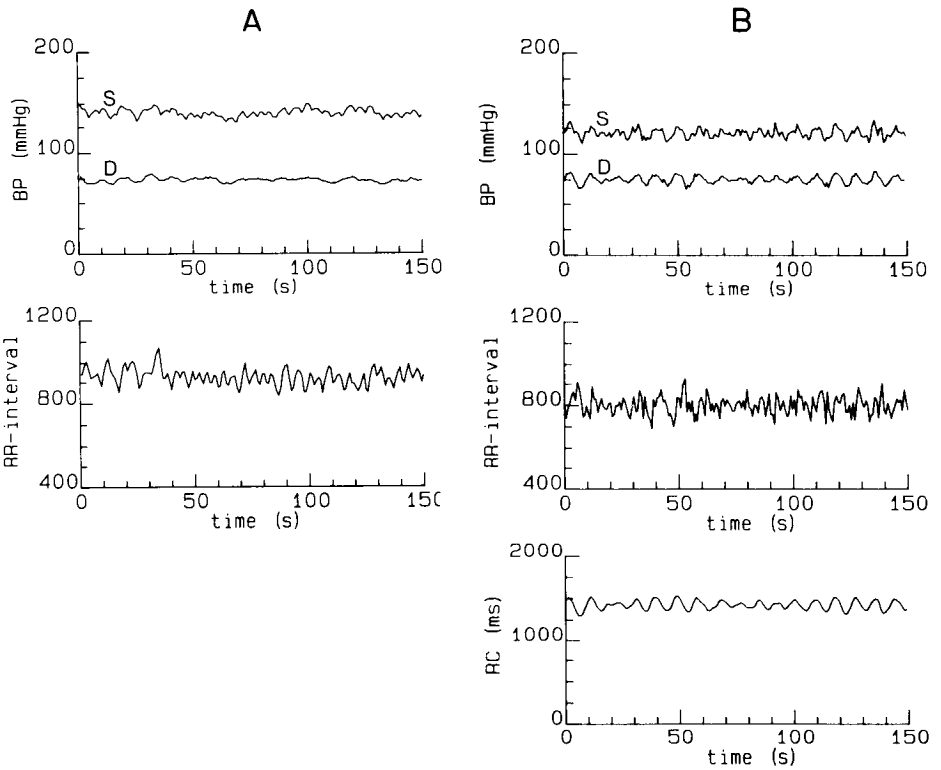

FIG. 4. *A*: blood pressure (BP) and R-R interval data from a young subject at rest. Respiratory variability and 10-s variability are present in systolic (S) values and intervals, but almost only 10-s variability is seen in diastolic (D) values. *B*: values of systolic and diastolic pressure, R-R intervals, and peripheral resistance [or actually arterial time constant (RC)] as obtained from simulations with our model. Note similarity with *A*.

frequency and has values between 0 (no relationship) and 1 (maximal relationship). The phase spectrum $\varphi(f)$ (solid line in Figs. 5*D* and 6*D*) has values between −180° and 180°. It indicates the lead or lag of one signal with respect to the other as a function of frequency. In our figures pressure variability leads interval variability if the phase is negative (e.g., at f = 0.1 Hz in Figs. 5*D* and 6*D*).

The main features of the spectra of actual data for the power spectra of pressure and R-R intervals are as follows (Fig. 5; cf. Refs. 9 and 27). *1*) A peak at the respiratory frequency is seen in the spectra of the R-R intervals (**I**, Fig. 5*A*), the systolic pressures (**S**, Fig. 5*B*), and the pulse pressures (**P**, Fig. 5*C*). The respiratory peak in the spectra of the diastolic pressures (**D**, Fig. 5*C*) is usually small or absent. *2*) A peak at the frequency of the 10-s rhythm is seen in all spectra, but it is often small in the spectrum of the pulse pressures (**P**, Fig. 5*C*). The main features of the spectra of actual data for the cross spectra of pressure against R-R intervals are as follows. *3*) A high coherence is found between pressure variations and interval variations around 0.1 Hz as well as at the respiratory frequency (Fig. 5, *D–F*). *4*) The phase spectrum of **S** against **I** (Fig. 5*D*) shows values of ~−70° at 0.1 Hz, i.e., pressure leads, and of ~0° at the normal respiratory frequencies (0.2–0.3 Hz). *5*) The phase spectrum of **D** against **I** (Fig. 5*E*) fluctuates around −90°. *6*) The phase spectrum of **P** against **I** (Fig. 5*F*) shows a small negative value around 0.1 Hz and a value of 0° for the respiratory frequencies.

Power spectra and cross spectra belonging to the simulated data are shown in Fig. 6, *A–F*. Comparison of the spectra in Fig. 6 with the spectra of actual data (Fig. 5) shows a good resemblance for the power spectra, the coherence spectra, and the phase spectra, as can be seen by checking the list of features above. Minor differences are the lack of coherence between interval variability and diastolic variability in the respiratory band and the slightly positive phase difference between pulse pressures and intervals in the 0.1-Hz band. The respiratory frequency is more constant in the model than in the actual data; this explains the narrower respiratory peak in the power spectra of Fig. 6, *A–C*. As mentioned before the frequency range below 0.05 Hz is not considered here.

Response to Simulated Phenylephrine Injection

As a second test of the model the simulated response is shown to an imposed increase of peripheral resistance (or actually an increase of the time constant $\mathbf{T} = \mathbf{RC}$) in time. Such an increase of peripheral resistance is experimentally induced by a phenylephrine injection and leads to an increase in BP followed by a baroreflex-mediated increase of length of the R-R interval. The ratio of interval increase ΔI to pressure increase ΔBP after a phenylephrine injection is clinically used as a measure of BRS (29, 33).

In this simulation experiment respiration or noise are not included in the model. We let the factor T* (*Eq. 3*) increase by 1,000 ms in a period of 10 s (solid line in Fig. 7*A*). For these values the results correspond with experimentally obtained curves (32). The resultant change in the time constant T_n and equivalently in the peripheral resistance $R_n = T_n/\mathbf{C}$ (we put $\mathbf{C} = 1$) is less than the change in T*, due to the closed-loop control system (Fig. 1), which counteracts the change in T_n. Figure 7*A* shows the response of peripheral resistance r of systolic pressure s and of R-R interval i. Note that the deviations from the operating points, not the absolute values, are given here.

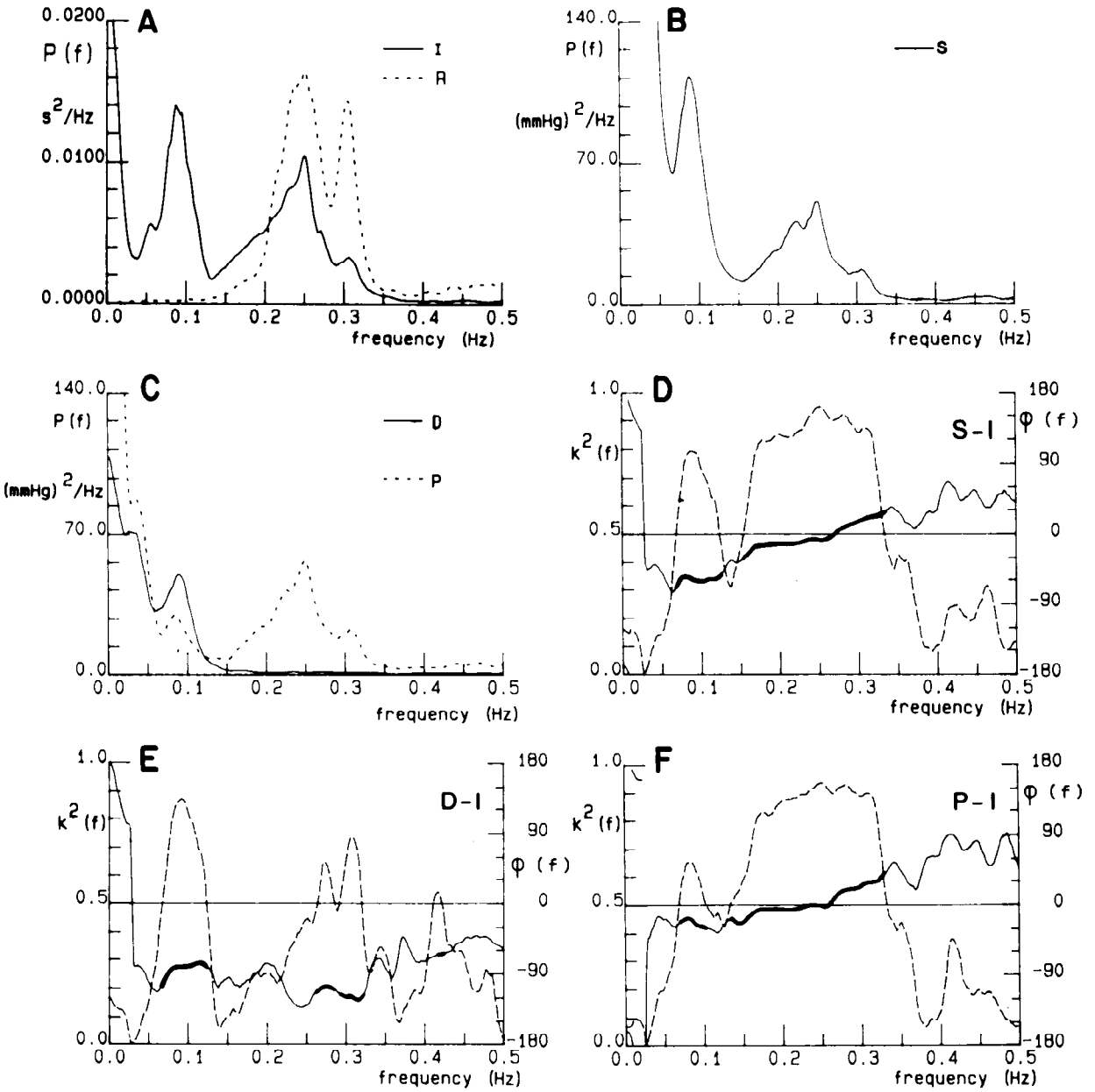

FIG. 5. Power spectra (*A–C*) and cross spectra (*D–F*) of blood pressure data and R-R interval data from a young subject (from Fig. 4*A*). *A*: power spectrum [P(f)] of intervals (**I**, *solid line*) and of respiration (**R**, *dashed line*). *B*: power spectrum of systolic pressures (**S**, *solid line*). *C*: power spectrum of diastolic pressures (**D**, *solid line*) and of pulse pressures (**P**, *dashed line*). *D–F*: squared coherence spectra [k^2(f), *dashed line*] and phase spectra [ϕ(f), *solid line*] of **S** against **I** (*D*), **D** against **I** (*E*), and **P** against **I** (*F*). Phase spectrum has negative values if pressure variability leads interval variability. If the coherence spectrum has a high value ($k^2 > 0.5$), phase spectrum is reliably estimated (*heavy solid line*).

In Fig. 7*B* the scatter plot of i_n vs. s_n (crosses) and of i_n vs. s_{n-1} (circles) is shown. The BRS is to be determined from the slope between pressure and interval values, but the literature is not unequivocal whether the plot of i_n vs. s_n or the plot of i_n vs. s_{n-1} should be considered for this purpose (18, 21, 28, 33).

The first beat is in the bottom left-hand corner of Fig. 7*B*; successive beats are upward to the right. The circled point is the new steady-state value. The line has a slope of 9 ms/mmHg, corresponding to vagal effects only. After a few beats the sympathetic effects become noticeable as an increase of the slope of the I vs. S curve. Both the plot of i_n vs. s_n and of i_n vs. s_{n-1} lead to a slope and hence an apparent BRS of ~10 ms/mmHg.

DISCUSSION

The presented beat-to-beat model of the CVS quantitatively describes the shape of the power spectra and cross spectra of BP variability and interval variability (see *Simulation of Resting Data*). The model also gives a good description of BP and interval response to an imposed increase of peripheral resistance as seen after the administration of phenylephrine (see *Response to Simulated Phenylephrine Injection*).

Recently Akselrod et al. (1) used spectral analysis techniques to study HR and BP data from awake dogs, but they considered only power spectra. In our opinion the present study shows that important information on

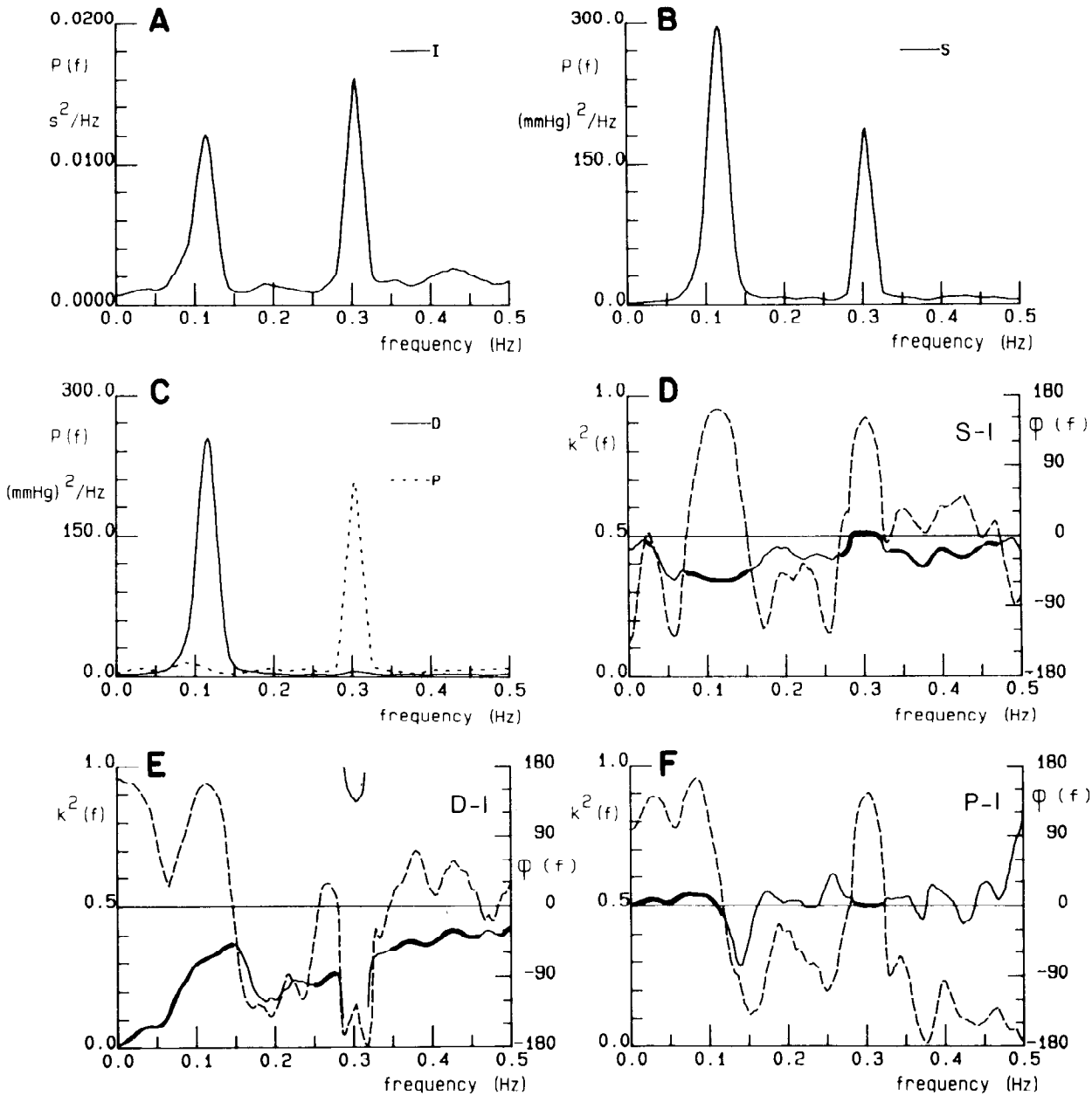

FIG. 6. Power spectra (*A–C*) and cross spectra (*D–F*) computed from simulated blood pressure data and R-R interval data. These spectra are to be compared with spectra from actual blood pressure data and interval data in Fig. 5. See Fig. 5 for definitions of abbreviations and symbols.

the relationship between HR and BP data can be derived from cross spectra and particularly from the phase spectra between interval variability and BP variability. Akselrod et al. (1) concluded from their pacing and blockade experiments that in the dog respiratory BP variability is secondary to respiratory HR variability. Our model suggests the opposite to be the case in resting humans: respiration first affects the cardiac output and hence the blood pressure, and next the vagal baroreflex transforms the respiratory BP waves into interval fluctuations. (The sympathetic branch of the baroreflex is not effective at these frequencies; cf. APPENDIX.) These assumptions lead to power spectra and phase spectra from simulated data (Fig. 6) that agree well with spectra from actual data (Fig. 5). Both in Fig. 6*D* and in Fig. 5*D* the phase between systolic pressure variability and R-R interval variability at the respiratory frequency (0.25 Hz) is approximately zero, as is to be expected if systolic pressure S_n determines the length of R-R interval I_n through fast vagal action (see Fig. 2). Such a phase of zero between S_n and I_n at respiratory frequencies was a constant finding in our actual data (9), and recently Pagani et al. (27) confirmed this value. Our analysis, however, cannot rule out the possibility that both BP and HR are independently affected by respiration in such a way as to mimic the above-described vagal control of HR.

The model makes it clear also why almost no variability in diastolic values is found at the respiratory frequency both in the spectrum of the actual data (solid line in Fig. 5*C*) and in the spectrum of simulated data (solid line in Fig. 6*C*) (10, 12). An increased value of the systolic pressure, if due to respiratory effects, would lead

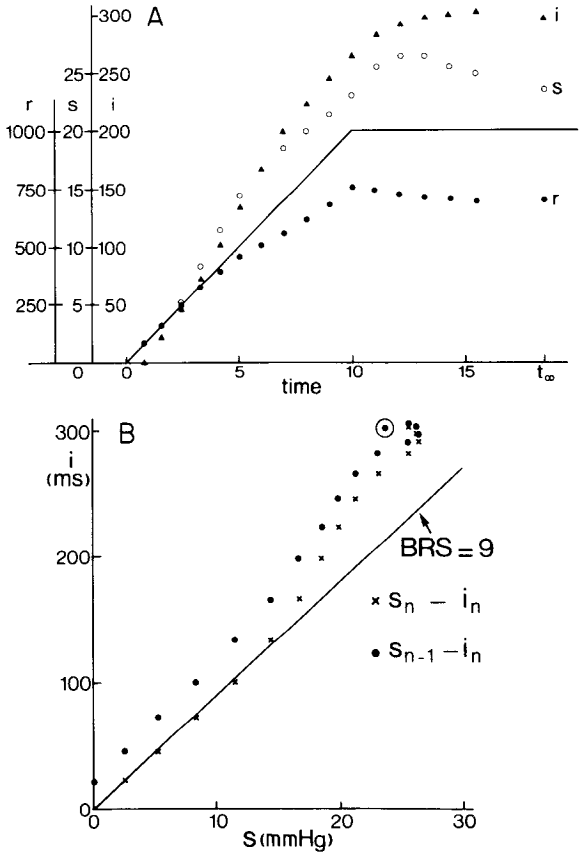

FIG. 7. *A*: simulated response of R-R interval (i, in ms; *triangles*), systolic pressure (s, in mmHg; *open circles*), and peripheral resistance (r, in ms; *filled circles*), or actually time constant (τ = rC with C = 1), to an imposed increase of peripheral resistance (*line*). Resulting increase in r at time t_∞ is smaller than imposed one due to negative feedback in cardiovascular system (cf. Fig. 1). (Note that deviations of interval, pressure, and resistance from their steady-state values are shown.) *B*: scatter plot of i_n vs. s_n (*crosses*) and of i_n vs. s_{n-1} (*filled circles*) derived from *A*. First beat is in *bottom left-hand corner*, and successive beats are *upward* to *right*. *Circled point* is new steady-state value. *Line* has a slope of 9 ms/mmHg, corresponding to only vagal control (cf. Fig. 3). BRS, baroreflex sensitivity.

to an increase of the next diastolic pressure. However, the increased systolic pressure induces a lengthening of the R-R interval and hence of the diastolic run-off period, which tends to decrease the diastolic pressure. It can be shown that these effects cancel each other when $a_0 = \tau/\mathbf{S}$, with a_0 as the BRS coefficient, τ as the time constant of the arterial Windkessel, and **S** as the mean systolic pressure (10, 11). For physiologically realistic values of these parameters this equality is approximately fulfilled (cf. DESCRIPTION OF THE MODEL), and thus the diastolic variability at the respiratory frequency is much less than the systolic variability.

The 10-s variability in HR and BP is in the model due to the delay in the sympathetic feedback loops. This amounts to the effect of a band-pass filter; noise ~0.1 Hz is amplified compared with noise at other frequencies (see APPENDIX). Other explanations of the 10-s rhythm have been put forward, e.g., the presence of an intrinsic 10-s oscillator in the central nervous system, which modulates the peripheral resistance by the sympathetic pathway (for a survey of possible mechanisms causing the 10-s rhythm see Ref. 23). The present paper shows, however, that realistic parameter values of the model are able to explain the 10-s rhythm without the need for an extra hypothetical oscillator. A similar result was obtained by Wesseling et al. (34, 36) using a continuous model of the CVS.

The phase of ~−70° at 0.1 Hz between systolic variability and interval variability in our model is due to the combined effect of vagal and sympathetic baroreflex regulation of the cycle length. At the respiratory frequency the phase difference between systolic pressure variability and interval variability is around zero because for these frequencies the slow sympathetic system is not effective, and only the vagal part of the baroreflex arc matters (see APPENDIX). The vagal control leads to a phase of zero. However, this argument is only qualitatively valid because it does not take into account the closed-loop properties of the system (6).

The response of the model to an imposed increase of peripheral resistance resembles experimental data (Fig. 7*A*). The upward concavity of the i_n vs. s_n curve (Fig. 7*B*) has been observed experimentally (18, 21). Note that in the model the concavity is not an intrinsic property of the relationship between BP and intervals but arises from the different dynamics of vagal and sympathetic contributions to the baroreflex arc. The amount of concavity can then be interpreted as a measure of the ratio of vagal to sympathetic control.

Figure 7*B* does not lead to an obvious preference for the use of the i_n vs. s_n curve or the i_n vs. s_{n-1} curve in the determination of the BRS. The slopes of both curves may be used to determine a BRS value of ~10 ms/mmHg. Note that the effect of noise and respiration is not taken into account in the simulation of Fig. 7. The results show that the BRS as measured by the administration of a pressure-increasing drug can hardly be characterized by a single number because it consists of a complex mixture of vagal and sympathetic effects. Indeed it is shown in the APPENDIX that the BRS should be considered as a frequency-dependent parameter.

A problem in modeling the CVS is that reliable values for the different parameters of the model (a_k, b_k, γ, and **T**) are scarcely found in the literature. However, we showed that physiologically acceptable values of these parameters lead to a quantitatively correct description of observed phenomena. We found, moreover, that the exact shape of the weighting function for the sympathetic baroreflex (Fig. 3) is not critical for the appearance of the results. This leads us to believe that the overall properties of the model tally to some extent with the actual CVS.

The model can be put to a test in several ways; e.g., in principle it is quite easy to simulate the effect of parasympathetic blockade in the model by putting a_0 to a small value. Simulated data from the model might then be compared with data from subjects in which a similar blockade is present. However, an important complication arises because vagal blockade in patients diminishes not only the vagally mediated variability (as is the case in the model), but it also diminishes the vagal tone, which determines the mean heart rate. In addition, because the model has heartbeats as time base the timing of physio-

logical events should be altered under these circumstances; e.g., the values of the parameters a_k and b_k would have to be adjusted to reflect the shorter duration of a beat.

The standard models of the human circulation do not consist of difference equations like the model we showed here but of differential equations (e.g., see Refs. 14, 15, 36). In these models the mean BP and a continuous HR signal are considered. If, however, short-term properties of the CVS are studied the fundamental discreteness of successive heartbeats cannot be neglected. Then it becomes advantageous to use a beat-to-beat representation of the CVS because an approach in continuous time can only be used if a very fine time scale is chosen in which each heartbeat remains observable (2). This implies a much more complicated model.

Our beat-to-beat model permits a physiological interpretation of power spectra and cross spectra of spontaneous BP and R-R interval fluctuations. A drawback of this approach is that there is no direct relationship with real time. This complicates the use of the model if HR increases above ~75 beats/min because the latency of the vagal baroreflex is such that under these conditions a systolic value does not affect the length of the present beat but of the following one (20).

In conclusion, our beat-to-beat model of the human CVS gives physiologically plausible explanations of respiratory sinus arrhythmia and of the 10-s variability in BP and HR. The model quantitatively explains both the spectra of HR and BP variability for data from resting subjects and the response of BP and HR to a phenylephrine-induced increase of peripheral resistance. How well the model describes data from subjects under other conditions is yet to be experimentally tested.

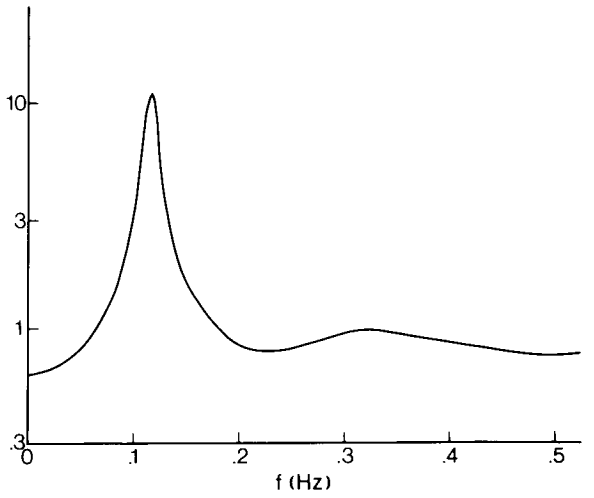

FIG. 8. Amplitude response of difference-equation model of cardiovascular system, considered as a band-pass filter of blood pressure variations. A sharp *peak* is seen at ~0.1 Hz, corresponding to 10-s variability in blood pressure and heart rate as observed in experimental data. *Horizontal axis*, frequency (f, in Hz); *vertical axis*, gain.

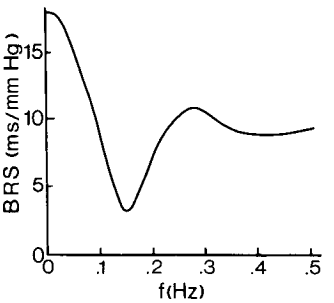

FIG. 9. Gain of the baroreflex arc or baroreflex sensitivity (BRS, in ms/mmHg) as a function of frequency (f, in Hz). For low frequencies BRS consists of sympathetic and vagal contributions but for high frequencies (above 0.2 Hz) consists almost only of a vagal contribution with BRS = 9 ms/mmHg.

APPENDIX

In this appendix we discuss some mathematical properties of the difference equations of our model. More details are given in Ref. 6.

10-Second Variability in Beat-to-Beat Model

For the chosen parameter values the equations of the model act as a band-pass filter of BP and HR variability with a pass band around 0.1 Hz. This is most easily seen by lumping *Eqs. 1–5* together in a single one. For small deviations from the operation point the difference between actual and effective pressure (*Eq. 1*) can be neglected, and one gets

$$s_n = K_0 s_{n-1} + \sum_{k>0} K_k\, s_{n-k-1} + \zeta_n \qquad (A1)$$

with $K_0 = \mathbf{D/S} + a_0(\gamma - \mathbf{D/RC})$, $K_k = a_k\,(\gamma\text{-}\mathbf{D/RC}) - b_k\mathbf{DI}/(\mathbf{RC})^2$, and ζ_n a noise contribution, consisting of the noise we added to *Eqs. 2′* and *4″* (*Simulation of Resting Data*) and respiratory influence. The filter characteristics of this equation can be found after z transformation (4, 16, 17)

$$s(z) = \zeta(z)/(1 - K_0 z^{-1} - \sum_{k>0} K_k z^{-k-1})$$

with $z = \exp(2\,\pi i\,\mathbf{I})$.

The shape of this filter for the parameter values used in RESULTS OF SIMULATIONS is given in Fig. 8. A sharp resonance peak exists at 0.1 Hz.

Equation A1 shows that as far as the filter properties are concerned the parameters a_k and b_k are related: even if $b_k = 0$ for all k (i.e., a constant peripheral resistance) the same filter characteristics can be obtained by adjusting the a_k's accordingly (and vice versa).

Frequency Dependency of Baroreflex

Because R-R interval i_n depends on a number of previous values of the systolic pressure s_{n-k} (k = 0–9; see *Eq. 2* and Fig. 3) the relationship between i_n and s_n is frequency dependent. Hence the BRS i_n/s_n cannot be characterized by a single number because it depends on the way s_n is changing. The value of the BRS as a function of frequency can be calculated by z transformation of *Eq. 2′*

$$i(z) = a_0 s(z) + \sum_{k>0} a_k s(z) z^{-k}$$

with $z = \exp(2\pi f\mathbf{I})$, and so

$$i(z)/s(z) = a_0 + \sum_{k>0} a_k z^{-k}$$

The value of the BRS i_n/s_n as calculated in this way is shown in Fig. 9. This figure shows the open-loop gain of the baroreflex arc, controling interval length. In contrast, Fig. 8 showed the filter characteristics of the whole CVS modeled as a closed-loop control system. The BRS equals $a_0 + \sum_{k>0} a_k$ = 18 ms/mmHg at f = 0 Hz, where vagal and sympathetic effects cooperate. For higher frequencies (~0.1 Hz) the BRS decreases because these

effects counteract. For still higher frequencies (>0.2 Hz) almost only the vagal action remains effective, and the BRS approaches the vagal value $a_0 = 9$ ms/mmHg.

We thank Ir. K. H. Wesseling, Ir. J. J. Settels, Dr. W. Wieling, and Dr. G. A. van Montfrans for practical support and critical comments during this study. W. Stok assisted in the preparation of the figures.

This study was supported by a grant from the Netherlands Organization for the Advancement of Pure Research (ZWO).

Received 22 April 1986; accepted in final form 25 March 1987.

REFERENCES

1. AKSELROD, S., D. GORDON, J. B. MADWED, D. C. SNIDMAN, D. C. SHANNON, AND R. J. COHEN. Hemodynamic regulation: investigation by spectral analysis. *Am. J. Physiol.* 249 (*Heart Circ. Physiol.* 18): H867–H875, 1985.
2. BENEKEN, J. E. W., AND B. DEWIT. A physical approach to hemodynamic aspects of the human cardiovascular system. In: *Physical Basis of Circulatory Transport: Regulation and Exchange*, edited by E. B. Reeve and A. C. Guyton. Philadelphia, PA: Saunders, 1967.
3. BORST, C., AND J. M. KAREMAKER. Time delays in the human baroreceptor reflex. *J. Auton. Nerv. Syst.* 9: 399–409, 1983.
4. BOX, G. P., AND G. M. JENKINS. *Time Series Analysis: Forecasting and Control.* San Francisco, CA: Holden Day, 1976.
5. COLEMAN, T. G. Mathematical analysis of cardiovascular function. *IEEE Trans. Biomed. Eng.* 32: 289–294, 1985.
6. DEBOER, R. W. *Beat-to-Beat Blood-Pressure Fluctuations and Heart-Rate Variability in Man: Physiological Relationships, Analysis Techniques and a Simple Model* (PhD thesis). Amsterdam: Univ. of Amsterdam, 1985.
7. DEBOER, R. W., J. M. KAREMAKER, AND J. STRACKEE. Beat-to-beat variability of heart interval and blood pressure. *Automedica Lond.* 4: 217–222, 1983.
8. DEBOER, R. W., J. M. KAREMAKER, AND J. STRACKEE. Comparing spectra of a series of point events, particularly for heart-rate variability spectra. *IEEE Trans. Biomed. Eng.* 31: 384–387, 1984.
9. DEBOER, R. W., J. M. KAREMAKER, AND J. STRACKEE. Relations between short term blood-pressure fluctuations and heart-rate variability in resting subjects. I. A spectral analysis approach. *Med. Biol. Eng. Comput.* 23: 352–358, 1985.
10. DEBOER, R. W., J. M. KAREMAKER, AND J. STRACKEE. Relations between short term blood-pressure fluctuations and heart-rate variability in resting subjects. II. A simple model. *Med. Biol. Eng. Comput.* 23: 359–364, 1985.
11. DEBOER, R. W., J. M. KAREMAKER, AND G. A. VANMONTFRANS. Determination of baroreflex sensitivity by spectral analysis of spontaneous blood-pressure and heart-rate fluctuations in man. In: *Neural Mechanisms and Cardiovascular Disease*, edited by B. Lown, A. Malliani, and D. Prosdocimi. Padua, Italy: Liviana, 1986, p. 303–315.
12. DEBOER, R. W., J. M. KAREMAKER, AND W. WIELING. Suppression of respiratory influence in the diastolic pressure as evidence of a functioning baroreflex in man (Abstract). *J. Physiol. Lond.* 366: 55P, 1985.
13. GOLENHOFEN, K., AND G. HILDEBRANDT. Die Beziehungen des Blutdruckrhythmus zu Atmung und peripherer Durchblutung. *Pfluegers Arch.* 267: 27–45, 1958.
14. GRODINS, F. S. *Control Theory and Biological Systems.* New York: Columbia Univ. Press, 1963.
15. GUYTON, A. C., T. G. COLEMAN, AND H. J. GRANGER. Circulation: overall regulation. *Annu. Rev. Physiol.* 34: 13–46, 1972.
16. JENKINS, G. M., AND D. G. WATTS. *Spectral Analysis and Its Applications.* San Francisco, CA: Holden Day, 1968.
17. JURY, E. I. *Theory and Application of the z-Transform Method.* Huntington, NY: Krieger, 1973.
18. KAREMAKER, J. M. *Vagal Effects of the Baroreflex on Heart Rate* (MD thesis). Amsterdam: Univ. of Amsterdam, 1980.
19. KAREMAKER, J. M. Short-term regulation of blood pressure and the baroreceptor reflex. In: *Psychophysiology of Cardiovascular Control,* edited by J. F. Orlebeke, G. Mulder, and L. J. P. VanDoornen. New York: Plenum, 1985, p. 55–68.
20. KAREMAKER, J. M. Cardiac cycle time effects: information processing and the latencies involved. In: *Psychophysiology of Cardiovascular Control,* edited by J. F. Orlebeke, G. Mulder, and L. J. P. VanDoornen. New York: Plenum, 1985, p. 535–548.
21. KAREMAKER, J. M., AND C. BORST. Measurement of baroreflex sensitivity in hypertension research. In: *Arterial Baroreceptors and Hypertension,* edited by P. Sleight. Oxford, UK: Oxford Univ. Press, 1980, p. 455–461.
22. KOCH, E. *Die Reflektorische Selbststeuerung des Kreislaufes.* Dresden, Germany: Steinkopf, 1931.
23. KOEPCHEN, H. P. History of studies and concepts of blood-pressure waves. In: *Mechanisms of Blood-Pressure Waves,* edited by K. Miyakawa, H. P. Koepchen, and C. Polosa. Berlin: Springer-Verlag, 1984, p. 3–23.
24. KORNER, P. I. Integrative neural cardiovascular control. *Physiol. Rev.* 51: 312–367, 1971.
25. MELCHER, A. Respiratory sinus arrhythmia in man: a study in heart rate regulating mechanisms. *Acta Physiol. Scand. Suppl.* 435: 1–31, 1976.
26. NOBLE, M. I. M., D. TRENCHARD, AND A. GUZ. Effect of changing heart rate on cardiovascular function in the conscious dog. *Circ. Res.* 19: 206–213, 1966.
27. PAGANI, M., F. LOMBARDI, S. GUZZETTI, O. RIMOLDI, R. FURLAN, P. PIZZINELLI, G. SANDRONE, G. MALFATTO, S. DELL'ORTO, E. PICCALUGA, M. TURIEL, G. BASELLI, S. CERUTTI, AND A. MALLIANI. Power spectral analysis of heart rate and arterial pressure variabilities as a marker of sympatho-vagal interaction in man and conscious dog. *Circ. Res.* 59: 178–193, 1986.
28. PICKERING, T. G., AND J. DAVIES. Estimation of the conduction time of the baroreceptor-cardiac reflex in man. *Cardiovasc. Res.* 7: 213–219, 1973.
29. PICKERING, T. G., B. GRIBBIN, E. S. PETERSEN, D. J. C. CUNNINGHAM, AND P. SLEIGHT. Effects of autonomic blockade on the baroreflex in man at rest and during exercise. *Circ. Res.* 30: 177–185, 1972.
30. ROSS, J., AND J. W. LINHART. Effects of changing heart rate in man by electrical stimulation of the right atrium. *Circulation* 32: 549–558, 1965.
31. SIMON, A. C., M. E. SAFAR, J. A. LEVENSON, G. M. LONDON, B. I. LEVY, AND N. P. CHAU. An evaluation of large arteries compliance in man. *Am. J. Physiol.* 237 (*Heart Circ. Physiol.* 6): H550–H554, 1979.
32. SLEIGHT, P. The physiology of heart-rate control by arterial baroreceptors in man and animals. In: *The Study of Heart-Rate Variability*, edited by R. I. Kitney and O. Rompelman. Oxford, UK: Clarendon, 1980, p. 107–116.
33. SMYTH, H. S., P. SLEIGHT, AND G. W. PICKERING. Reflex regulation of arterial pressure during sleep in man: a quantitative method of assessing baroreflex sensitivity. *Circ. Res.* 24: 109–121, 1969.
34. WESSELING, K. H., AND J. J. SETTELS. Baromodulation explains short term blood-pressure variability. In: *Psychophysiology of Cardiovascular Control,* edited by J. F. Orlebeke, G. Mulder, and L. J. P. VanDoornen. New York: Plenum, 1985, p. 69–97.
35. WESSELING, K. H., J. J. SETTELS, G. M. A. VANDERHOEVEN, J. A. NIJBOER, M. W. T. BUTUIN, AND J. C. DORLAS. Effects of peripheral vasoconstriction on the measurement of blood pressure in a finger. *Cardiovasc. Res.* 19: 139–145, 1985.
36. WESSELING, K. H., J. J. SETTELS, H. G. WALSTRA, H. J. VANESCH, AND J. J. DONDERS. Baromodulation as the cause of short term blood pressure variability? In: *Proceedings of the International Conference on Application of Physics to Medicine and Biology Trieste 1982,* edited by G. Alberi, Z. Bajzer, and P. Baxa. Singapore: World Scientific, 1983, p. 247–276.